Colloids and Surfaces A 564 (2019) 152–160

Contents lists available at ScienceDirect

Colloids and Surfaces A

journal homepage: www.elsevier.com/locate/colsurfa

Preparation and characterization of temperature-triggered silica microcapsules containing sodium monofluorophosphate with tolerability to extreme pH

Qiqi Qu[a,b], Hua Wang[a,*], Jing He[a,b], Zheng Su[a,b], Tengfei Qin[a,b], Xingyou Tian[a]

[a] Key Laboratory of Photovoltaic and Energy Conservation Materials, Institute of Applied Technology, Hefei Institutes of Physical Science, Chinese Academy of Sciences, Hefei, 230031, PR China
[b] University of Science and Technology of China, Hefei, 230026, PR China

GRAPHICAL ABSTRACT

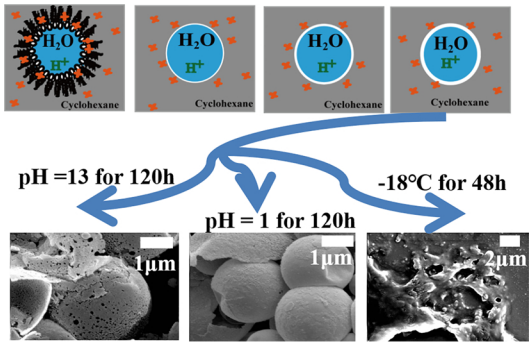

ARTICLE INFO

Keywords:
W/O emulsion
Capsule
Sodium monofluorophosphate

ABSTRACT

Low porosity silica microcapsules (SiO_2/Sodium monofluorophosphate) were synthesised by a soft-template method in room temperature. Morphology of silica microcapsule can be controled by changing the concentration of TEOS in reinforcement phase in the range of 1%–4%. With the increased concentration, thickness of capsule raised and some rod-like structures occured. The impacts of oil phase volume fraction and rotation speed of emulsification on the diameter distribution of capsules were discussed. The former functioned via changing viscosity of mixed solution while the latter played a complicated role in diameter distribution. This method of microencapsulation used in our paper is easy to achieve for that the experimental conditions are mild and do not require complicated or costly instruments, which is suitable for industrial production. In addition, we also explored the changes of microcapsules under different environmental factors including temerature and pH.

1. Introduction

Reinforced concrete has become a worldwide building material, due to its excellent mechanical behavior and economic price [1]. The extremely alkaline environment provided by the concrete causes a protective film on the surface of the reinforcement bar, which is of great benefit to the durability of reinforced concrete structure. However, under the marine environment, the factors just like moisture, chloride

* Corresponding author.
E-mail address: wanghua@issp.ac.cn (H. Wang).

https://doi.org/10.1016/j.colsurfa.2018.11.057
Received 29 September 2018; Received in revised form 24 November 2018; Accepted 25 November 2018
Available online 26 November 2018
0927-7757/

ions and carbon dioxide destroy the protective film [2], and cause corrosion of the steel reinforcement, which will lead to a significant decrease of the building service life by affecting the concrete structural performance. One of the powerful measures to solve above problems is using corrosion inhibitors [3]. Some chemicals are able to play a valuable role in slowing down corrosion rate. There are two ways to put those drugs into use: one is brushing inhibitors onto the surface of reinforced concrete structures; another is directly adding inhibitors into the cement mortar before concrete sets [4].

Sodium monofluorophosphate(MFP) [5], a water-soluble inorganic corrosion inhibitor, was noted for its environmentally friendly character. Just like what we mentioned above that we may apply MFP to concrete by adding them directly in concrete or painting on surface. However, the reaction between concrete matrix and anion of MFP happened quickly, especially in the water environment [6].

Considering such reaction, on the one hand, MFP improves the concrete's compactness and on the other hand inhibits the migration efficiency of drugs by reason of that MFP is unable to reach the steel surface (Chemicals reacted with concrete too early). Only the MFP that reached to the surface of steel bar can play the role of rust inhibitor. Therefore, it is necessary to increase the water resistance and to make sure the drug migrate to surface of rebar as much as possible.

Putting chemicals in nano-size or micro-size capsules is an efficient technology to protect active medicine and implement some new functional applications [7]. In recent decades, with the booming development of microencapsulation technology in bio-materials, medicine [8], cosmetics [9], and food fields [10], researchers has also applied it to concrete. In the previous papers, shell of the microcapsules is mostly composed of polymers. Admittedly, there are many advantages by using polymer as the outer shell. However, in a highly alkaline environment, it is possible that some unpredictable chemical reactions between organic wall materials and components of concrete may happen and which would have a bad infuluence on the structural performance of concrete. Jiandong Zuo et al. prepared Polystyrene (PS)/sodium monofluorophosphate (MFP) microcapsules by W/O/W solvent volatilization method. PS/MFP microcapsules showed positive sustained release properties in simulated concrete solution. Later they prepared polylactic acid/sodium monofluorophosphate microcapsules by spray drying and focused on the impact of processing technology on microcapsules [11,12]. Biqin Dong et al proposed a kind of microcapsule which used ethyl cellulose (EC) as the shell and the rust inhibitors $NaNO_2$ and MFP as inner contents, exhibited chemical self-healing properties by delaying the depassivation of the rebar and reducing the corrosion rate in the mortar [13]. SiO_2 is original component belongs to concrete and has good compatibility with the concrete matrix. Waste materials such as pozzolan [14], glass cullet [15] which are mainly made up of silica are used invariably as raw materials for concrete. Both nano-scale and micro-scale SiO_2 can improve the durability of concrete [16].

This paper applied a W/O emulsion templating method to directly package MFP by dissolving MFP in aqueous phase before emulsification. TEOS was selected as silicone precursor for it is inexpensive and available which led to the forming of shell materials. Compared to hard template method, exploiting the W/O emulsion templating method can be more convienent owing to no process of removing template [17]. Moreover, this approach is gentle in reaction which could sustain at room temperature, and does not require complicated operations or expensive equipments. Therefore, there exist the potential for industrial application behind such fabrication method. We have read many valuable details which used the W/O method to synthesize silica capsule in the previously reported literature [18,19] while investigation about the effects of processing technology just occupied a spot of words. This article focuses on the synthesis process, in order to provide a certain reference for large-scale production. The morphology and thickness of capsules were affected by concentration of TEOS and multiple additions. Technological parameters obviously affect diameter distribution of microcapsules during emulsion formation and growth of outer wall. The effects of emulsifying speed and formula on microcapsules were also discussed. These microcapsules keep the shape integrity under severe acid and alkali corrosion conditions. In addition, due to the internal liquid/outer solid structure, microcapsules exhibited temperature responsiveness that under low temperature samples turned to rupture and release more drugs.

2. Materials and methods

2.1. Raw materials

Tetraethyl orthosilicate(TEOS), Cyclohexane, Sodium monofluorophosphate, Span80, Tween80 and HCl were obtained from Sinopharm Chemical Reagent Co., Ltd. Deionized water produced by laboratory. All of the reagents were used as received.

2.2. Preparation of solution

The preparation procedure has a litter changes on the base of W/O emulsion template method proposed by Shane P.Meaney et al [18]. The oil phase is cyclohexane solution containing 1% TEOS and 1% Span80. The 2 g TEOS and 2 g Span80 were dissolved in 196 g cyclohexane, and the total volume of solution is approximately 250 mL. The reinforcing solution is similar to oil phase without span80. The aqueous phase is acid solution. 0.75 g Tween80 and 1 g sodium monofluorophosphate were dissolved in 0.1 M HCl solution, and the total volume of this mixture solution is 50 mL. Do some adjustment with the 1 M hydrochloric acid solution to make sure final pH is equal to 2. The acid environment of water phase is beneficial to hydrolysis of TEOS.

2.3. Synthesis of MFP/SiO_2 microcapsule

The aqueous solution was added to the organic in volume ratio 1:10, 1:15 or 1:20 and emulsified at 10,000 RPM, 13000RPM or 16000RPM for 1 min. The emulsion was stirred with magnetic mixer at room temperature for 24 h to obtain the primary template which was named MFP/SiO_2-1. Reinforcement was performed by repeated addition of the 1% TEOS followed by an ageing period: a cyclohexane solution containing 1% TEOS was added to the primary template solution, and the primary capsules were modified by stirring at room temperature for another 24 h to obtain microcapsules named MFP/SiO_2-2. Comprehensive details about the name of samples and other terms are recorded in Table S1 in Surpporting Information.

According to the accumulation of previous researcher [20–23], two steps are involved in the silica growth process which are described with below chemical equations: one is the hydrolysis of TEOS and the other is the condensation of SiO_2 onto the seed surface. The whole process are also evealed in Fig. 1.

$$Si(OC_2H_5)_4 + 4H_2O \rightarrow Si(OH)_4 + 4C_2H_5OH \quad (1)$$

$$Si(OH)_4 \rightarrow SiO_2\downarrow + 2H_2O \quad (2)$$

2.4. Characterizations

Sirion-200 (FEI, America) scanning electron microscopy (SEM) was used to observe the morphology of capsules with gold coating. The sample was resuspended in ethanol and a small quantity deposited on silicon wafer and air dried before analysis. A transmission electron microscope (JEM-2100, TEM) was used to analyze the microstructure of the sample at 200 kV. Philips X' Pert Pro MPD X-ray diffractometer (40 kV, 40 mA) with Cu-Ka radiation (λ = 0.154 nm) was used to take the X-ray diffraction(XRD) measurements. Infrared (IR) spectra were recorded on a L 1,600,400 Spectrum TWO DTGS spectrometer made in Liantrisant, UK using ATR accessory method. Size distribution

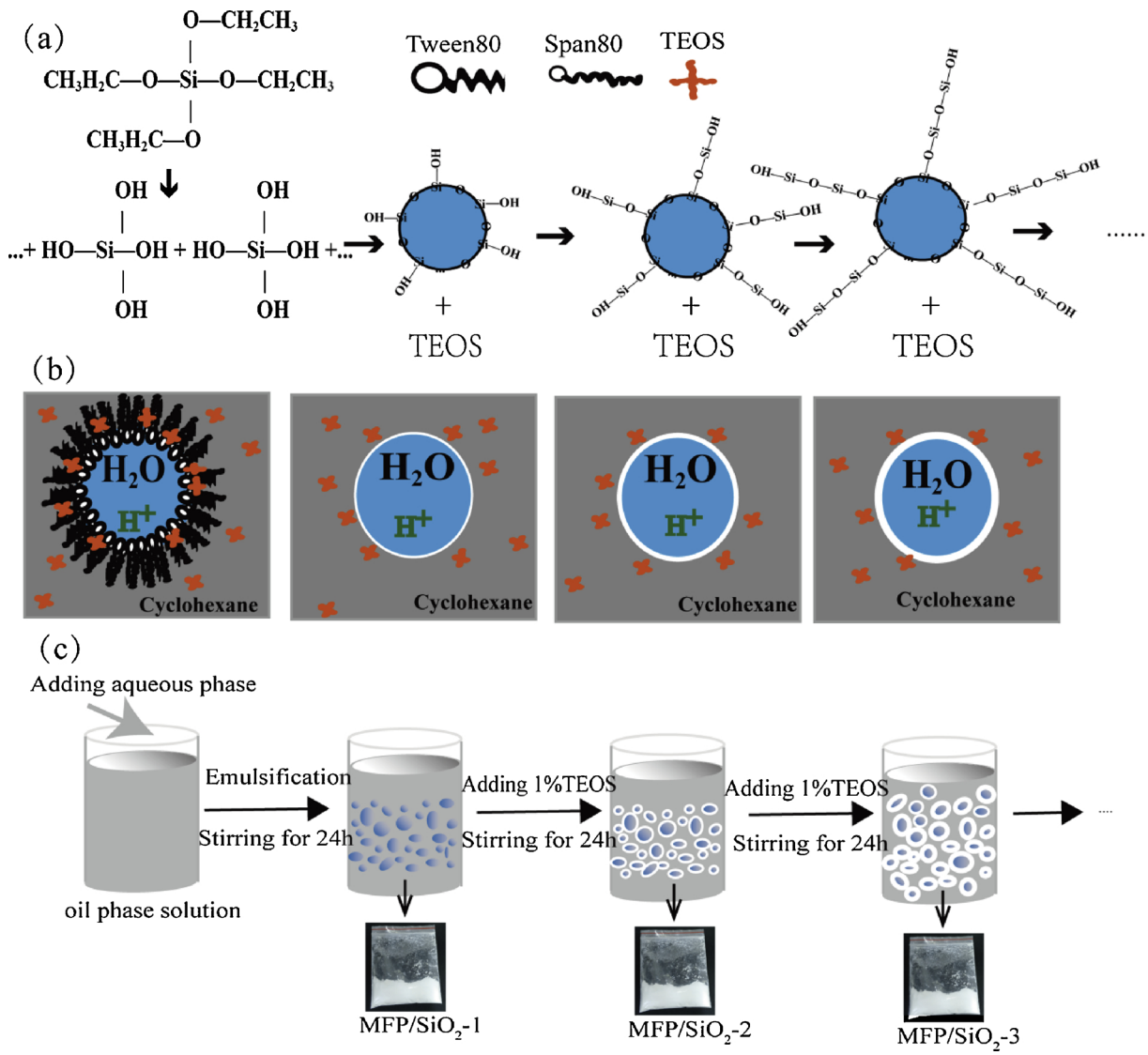

Fig. 1. Illustration of the procedures for preparation the MFP/SiO_2 capsules.

measurements were carried out via using a Malvern zetasizer 3000HSA. Every sample was tested at least 3 runs. Surface area and pore size analysis were performed using a BELSORP MINIIISpecific surface area and pore size measurement system with nitrogen adsorbate. Samples were calcined at 600 °C for overnight to remove any remaining organic components. InductivelyCoupledPlasma-AtomicEmissionSpectrometry (ICP-AES,Optima 7300DV) from PerkinElmer corporation was used to determine the content of P and Na in solution. Samples were dispersed in aqueous solution (acidic, alkaline or neutral) for some hours, then filtered with microporous membrane and diluted (Dilution factor can be found in supporting information) before measurement.

3. Results and discussion

3.1. Morphology

The multiple additions of silicon precursors are necessary to synthesis silica capsule. It is obviously that with the repeated reinforcements, the capsule became spherical and complete which can be find from the Fig. 2a–d. In Fig. 2a–b, capsules were flat and even broken because the inner materials outflowedAfter twice reinforcements, capsules showed a good spherical morphology. To improve the water resistance of inner drugs, we must reinforce the capsule more than two times. The surface of microsphere is a litter rough (below photo in Fig. 2f) for the reason that nano-SiO_2 provided by hydrolysis reaction of TEOS stacked one by one.

What deserves to be mentioned is that we can observe several hemispherical capsules in the more high magnification SEM pictures (Fig. 3b). Those broken containers demonstrated the exist of hollow silica capsule and the huge potential for loading drugs. TEM also proved that capsule is hollow. What we can detect is a translucent microspheres with distinct border in upon photo for Fig. 3. The black thin area refers to capsule's shell.

On the other hand, the concentration of TEOS in reinforcement phase also provide manifest effect on morphology of silica microcapsule. State of hollow capsule can be easily converted by adjusting concentration from 1% to 4%. Lower concentration guides the synthesization of abundant regular spherical capsules. With the concentration at 1% and 2%, microcapsules maintained clear translucent and the dark area which referred to the capsules' wall was also distinct (Fig. 4a and b). Raising concentration is one of the convient control measures for changing thickness of spherical shell, thickness have risen approximately by 40% from 46.92 ± 16.17 nm at 1% TEOS to 65.74 ± 17.07 nm at 2% TEOS. While, solid sphere under high concentration can be observed and rod-like structure product appeared. In order to get the capsules which we really required, preparation

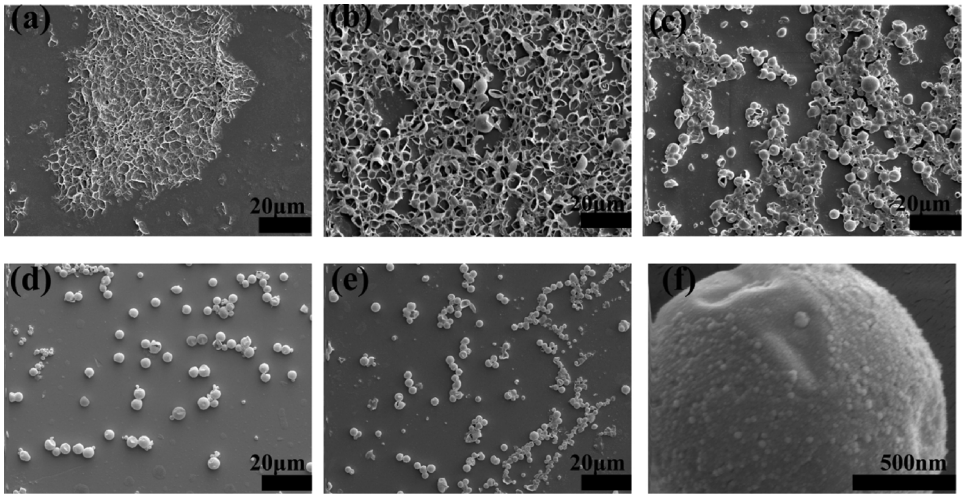

Fig. 2. The morphology SEM images of the capsules (a) MFP/SiO_2-1,(b) MFP/SiO_2-2, (c) MFP/SiO_2-3, (d) MFP/SiO_2-4, (e) MFP/SiO_2-5, and (f) rough surface of capsule.

principle that adding reinforcement phase contained low concentration TEOS with multiple times should be followed.

3.2. Compositions

There were many Si-O-Si bonds for that the outer shell of the microcapsules was formed by sol-gel reaction which were found at 1077 cm^{-1} (a broad and strong absorption peak marked by the dashed rectangle); There are many absorption peaks that are not part of the blank capsule, which should be the role of MFP. The pure MFP (dried overnight at 60 °C before the test) displayed a strong infrared absorption peak at 1157 cm^{-1} due to P═O stretching vibration absorption. For MFP/SiO_2, only one peak in the range of 1157 cm^{-1} to 1077 cm^{-1}. It can be traceable to merger of wide strong band from Si-O and weak band from P═O. The absorption peak of the MFP/SiO_2 capsule at 990 cm^{-1} corresponded to the absorption of pure MFP at 1005 cm^{-1}, caused by P—F stretching vibration. Symmetrical stretching vibration of $PO3^{2-}$ exhibited multimodal peaks from 1000 cm^{-1} to 500 cm^{-1} which corresponded to the absorption of the MFP/SiO_2 capsules at 916 cm^{-1}, 734 cm^{-1}, 616 cm^{-1} and 562 cm^{-1}. The presence of these peaks demonstrated exsit of MFP in microcapsules.

The physical states of the capsule and drug sodium monofluorophosphate were additionally investigated using the XRD techniques. As it may be seen in the Fig. 5(b) pure sodium

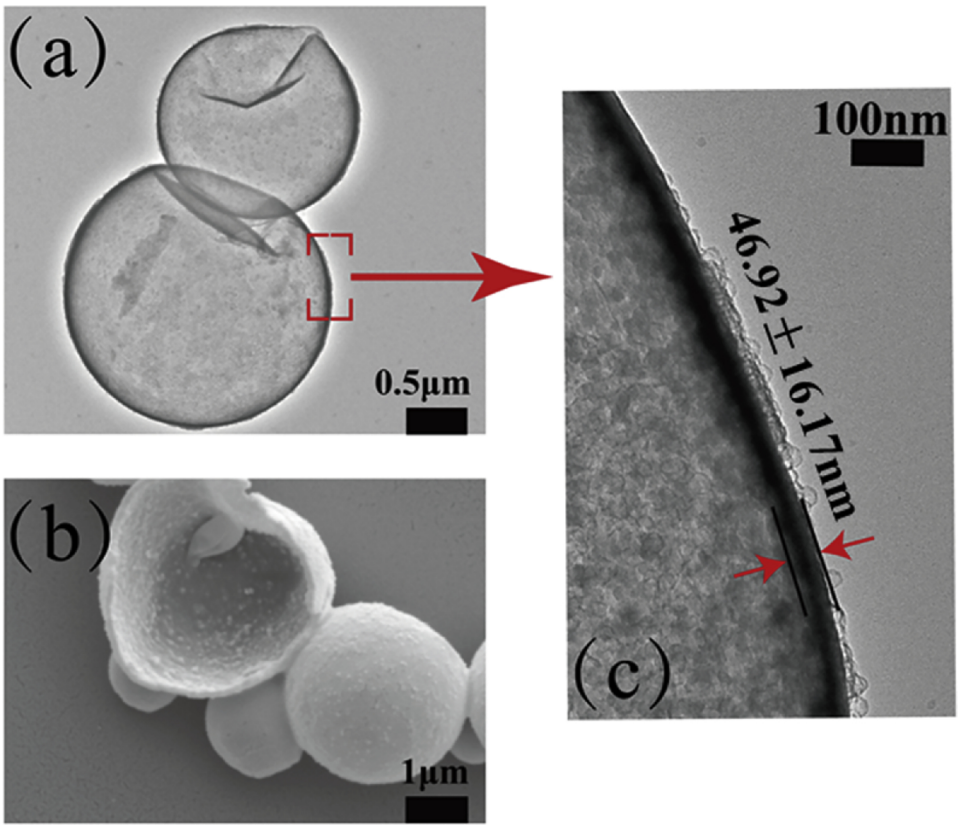

Fig. 3. (a) The TEM image of capsule; (b)SEM image of hollow structure and (c) thickness for silica capsule at 1%TEOS.

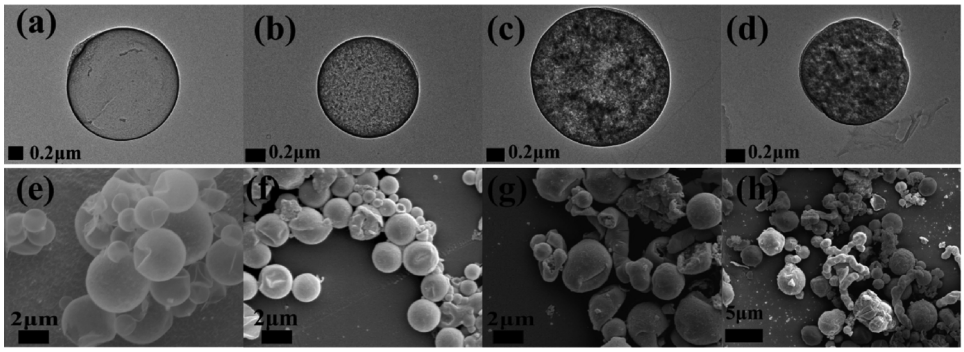

Fig. 4. TEM images of the capsules formed by (a)1%TEOS, (b)2%TEOS, (c)3%TEOS, (d)4%TEOS; SEM images of the capsules formed by (e)1%TEOS, (f)2%TEOS, (g) 3%TEOS, (h)4%TEOS.

monofluorophosphate exhibits the characteristic of crystalline bonding, there are many diffraction peaks of MFP. However, according to the X-ray powder diffraction peak curve of microcapsule, experimental product is amorphous for that there is only one dispersing diffraction peak in the range of 20 to 25 degrees. Taking into account that amorphous silica has a taro-like peak in the high angle range, such situation indicates that sodium monofluorophosphate dissolved in deionized water was encapsulated. EDS was used to analyze the elemental composition of microcapsules. The EDS spectrum of the composite capsules demonstrated that a large number of Si, O, and P, Na, F atoms were contained, proving that the capsule was built up by silica and monofluorophosphate was packaged. A small amount of Cl might come from the original solution, which was added before emulsification. And fewer C atoms can be traced back to the by-product ethanol produced when silica shell formed ($Si(OC_2H_5)_4 + 4H_2O \rightarrow Si(OH)_4 + 4C_2H_5OH$).

3.3. Porosity

Porosity were quantitatively examined using nitrogen gas sorption. This provides insight into the surface area and pore distribution of the synthesized material. The isotherm for the double reinforcement (MFP/SiO_2-2) is of type III as defined by IUPAC, while it converted to type II for triple and above reinforcement with the distinct point-B (MFP/SiO_2-3 and MFP/SiO_2-4) [24]. The reversible Type II isotherm is the normal form of isotherm obtained with a macroporous adsorbent. The reversible Type III isotherm, is the form of isotherm obtained non-porous, does not exhibit a Point B (Fig. 6a). In addition to this behavior, there was decreasing for surface area and total pore volume (Table 1). Above behaviors suggested that capsules were dense and close to non-porous for silica condensation had completed in initial reinforcement, and with the addition for TEOS after double reinforcement, increased surface

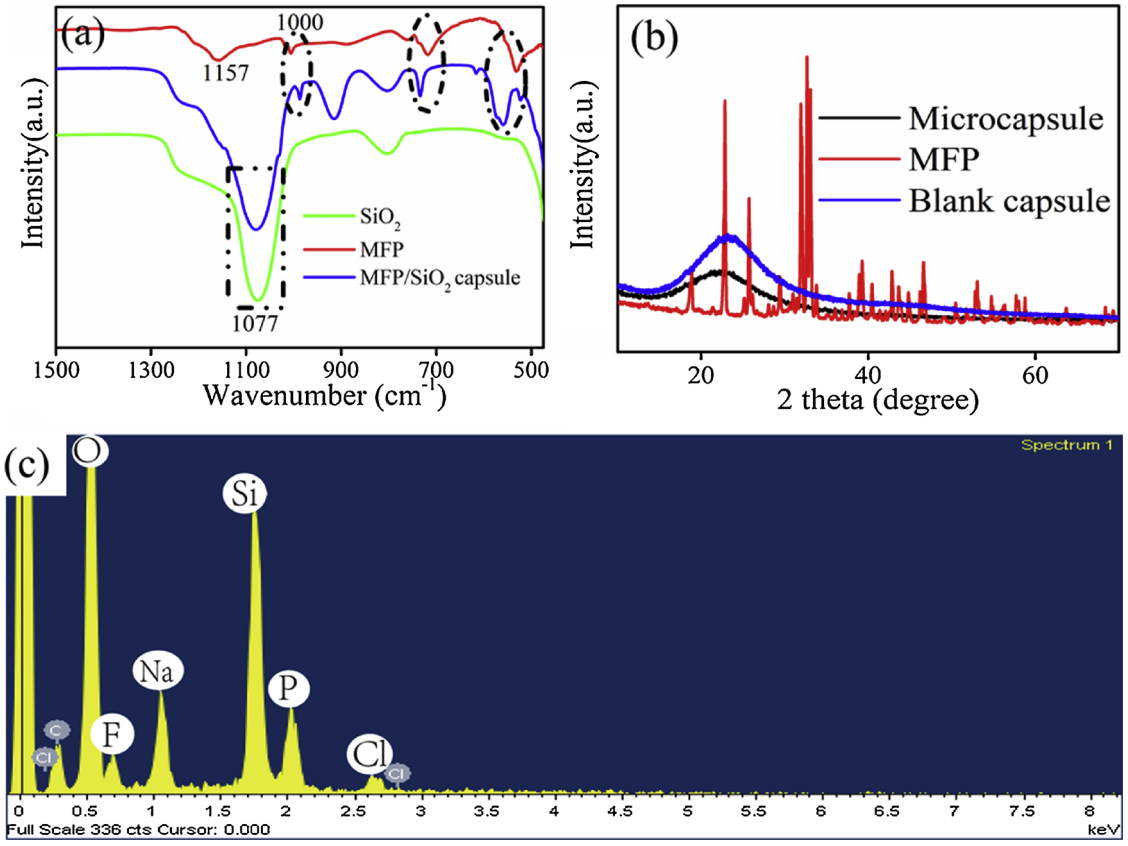

Fig. 5. (a) FT-IR spectra of capsules without MFP (green line), MFP/SiO_2 capsules (blue line) and pure MFP (red line refers, dried overnight at 60 °C before the test); (b)The XRD patterns of pure sodium monofluorophosphate (dried overnight at 60 °C before the test), blank capsule and microcapsule; (c) Energy dispersive spectrometry for MFP/SiO_2 microcapsule (For interpretation of the references to colour in this figure legend, the reader is referred to the web version of this article).

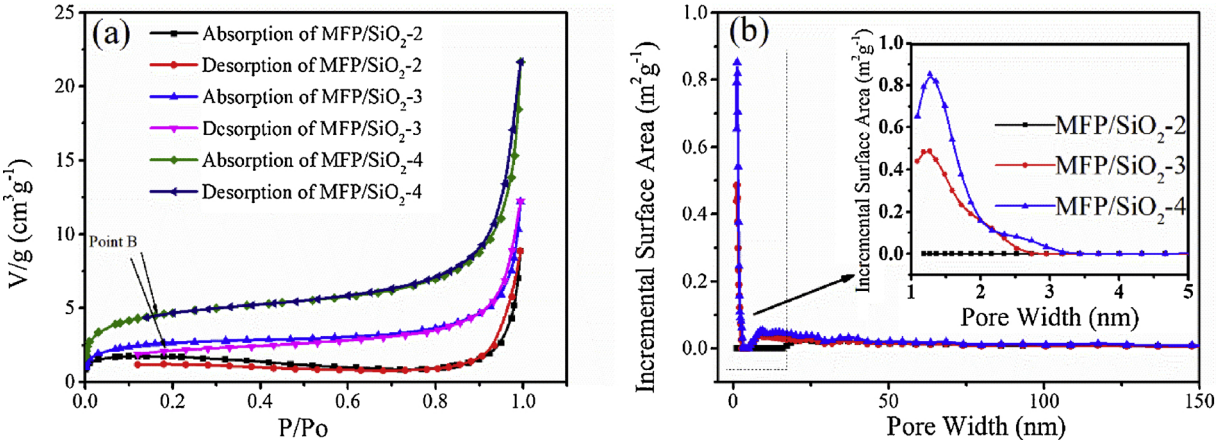

Fig. 6. (a) Nitrogen adsorption and desorption isotherms of MFP/SiO_2 capsules and (b) Contribution of the corresponding pore width to surface area.

Table 1
Data about pore of capsules.

Sample	MFP/SiO_2-2	MFP/SiO_2-3	MFP/SiO_2-4
BET Surface Area(m^2g^{-1})	7.0726	10.0808	17.2162
Langmuir Surface Area(m^2g^{-1})	7.9368	26.0756	49.9488
t-Plot Micropore Area(m^2g^{-1})	8.3755	4.4767	6.2761
Total Volume in Pores(cm^3g^{-1})	0.01319	0.01694	0.02468

area was observed owing to silica deposition onto the outer surface of the consolidated shell. The incremental surface area (Fig. 6b) indicated that continued addition beyond MFP/SiO_2-2 resulted in more and more micropores which increasingly dominated the surface area and total pore volume measurement. However, after multiple reinforcements, the surface area and porosity still remain in a low level which is benefit for microcapsules to retain cargos.

3.4. Diameter distribution

Many factors affects the diameter of microcapsules. In our study, we focus on emulsifying rate and volume fraction of continuous phase. In practice, those conditions for production are easier to control compared to others. To research the role that above two factors played is of great theoretical significance and application value to guide the industrial production. The MFP/SiO_2 capsules prepared by soft template has wide distribution dispersity than hard template method. After emulsification, there are numberless droplet in continuous phase. Adding TEOS thicken the wall of microcapsule by sol-gel reaction. However, the total diameter is much larger than the thickness of shell in length. The thickness of wall is about 46.92 ± 16.17 nm (Fig. 3c) while diameter of capsule is always above 1000 nm. In general, such contribution of shell to diameter can be ignored. It is realized that there were two stages in the progress of emulsion droplet formation:

(1) After that mixture was homogenized at 10,000 RPM or higher rate for 60 s, dispersed phase was broken into many tiny droplets. These primary tiny droplets had a significant impact on final size distribution.
(2) During the constantly stirring at a low rate, tiny droplets moved randomly and re-coalesced to be new bigger droplets. What's more is the TEOS in cyclohexane gathered at the interface between oil phase and water phase could hinder the further re-coalesce of small droplets by sol-gel reaction. Emulsifiers also conduced to stabilize the emulsion. The final diameter distribution was the result of above two stages.

3.4.1. Volume fraction of organic solution

The size distribution of microcapsule synthesized by emulsion method is always wide compared to hard template method. In order to understand clearly the trend, D25, D50, D75, D90, which were counted by cumulative distribution curves in Fig. 7b were exhibited in Fig. 7c. D50 is usually used as the average diameter of particles in the laser scattering particle analysis. Dmost means the most probable diameter which refers to the diameter value corresponding to the highest peak in the curve (Fig. 7a). The average diameter D50 of microcapsules was approximately 2.21 μm with lower volume ratio 10 (volume fraction of continuous phase is 90.91%), and rose to 3.07 μm with higher volume ratio 20 (volume fraction of continuous phase is 95.91%). With the increased volume fraction of continuous phase, diameter had clearly growth owing to decreased viscosity.

Just as previous reseachers reported in their papers, emulsions always show a strong dependency of viscosity on the phase concentrations. Relative viscosity be used for describing the mixture viscosity. The theory of emulsion viscosity was first proposed by Taylor who derived the following equation [25]:

$$\eta_r = 1 + \frac{\eta_m + 2.5\eta_d}{\eta_m + \eta_d}\varphi$$

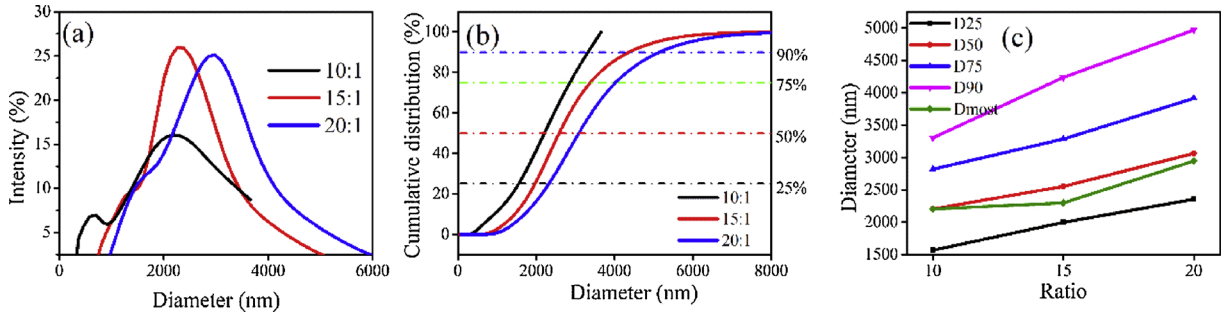

Fig. 7. Curves of (a) diameter distribution, (b) cumulative distribution, and (c) diameter versus ratio of oil and water.

Where η_r is relative viscosity, η_m is the viscosity of a continuous medium, η_d is viscosity of liquid dispersed droplets and φ is the volume concentration of dispersed particles (irrespective of their sizes). This equation demonstrated that with the reduced aqueous phase (raised oil phase), viscosity of mixture increased. Normally, volume fraction of continuous phase over 76%, there must be W/O emulsion. With the volume fraction rising, the mixture viscosity will down. The coalescence efficiency escalated for that the declined viscosity encouraged movement of tiny droplets. While in practice, correspondence between viscosity and volume fraction would not be such perfect linear relationship. The volume concentration of dispersed particles was also related to the size and distribution of the dispersed particles. Although high volume fraction of continous phase led to low viscosity is certain [26], and low viscosity directed make formation of large droplets is ture [27]. From above formula, we can know that it is not a simple linear relationship between viscosity and oil phase. However, without a doubt, there is a strong positive correlation between aqueous phase and viscosity. With the oil phase increased which equals to ratio of oil and water from 10 to 20, the viscosity of emulsion reduce. So that tiny droplets move faster result in more big droplets.The phenomenon displayed in Fig.7c could be explained well that the most probable size of capsule and other types of diameter all increase.

3.4.2. Rotation speed of emulsion

It is worth mentioning that bimodal DSD was observed, and the same phenomenon had been reported in previous articles [28]. We defined “large” as the number of particels which corresponding to right peak for every distribution curve. And the “small” refers to left peak for every distribution curve. Associated datas were recorded in Fig. 8d. Many studies have shown that high rotational speeds produced more small droplets. This trend can be attributed to an increase in energy dissipation rate caused by an increase in rotor speed, resulting in rupturing large droplets [29]. Interestingly, with increased rotation speed, diameter of capsules did not fall down as predicted before. Diameter value at 13,000 rpm was larger than 10,000 rpm. This may attribute to that capsules prepared at 16,000 rpm under 1000 nm in diameter were approximately 70% (only 10% for 10,000 rpm, 3% for 13,000 rpm). Such emulsion system exhibited certain properties of submicron emulsions. A microemulsion is thermodynamically stable, whereas a ordinary emulsion is not. And the thermodynamically stability of submicronemulsion is somewhere in between. In the emulsion system, tiny droplet tended to coalesce into large one to decrease surface energy. The ordinary emulsion prepared at 13,000 rpm was more abundant in number of tiny droplets than which at 10,000 rpm. The probability of collision between small droplets is greater at 13,000 rpm than which at 10,000 rpm. Therefore, we can explain the upward trend of diameter value in Fig. 8c for the risen coalescence efficiency. The emulsion prepared at 16,000 rpm is relatively more stable, and the trendence of coalescence was not manifest. Hence, such an emulsion system better maintained the initial particle distribution characteristics of droplets. Increased speed led to growing number of tiny droplets. The coalescence efficiency of droplets effected the number of big droplets. When the stirring speed was slow (from 10,000 rpm to 13,000 rpm), impact of coalesce was evident. In turn, when the stirring speed rise to 16,000 rpm, the tendency of coalescence was unconspicuous. Thus, we can explain the trend that why the value of most probable diameter and other type of diameter be maximum at 13,000 rpm. In general, the effect of rotation speed on particle size was still obvious, which increased the number of small droplets in the system and reduced the number of large droplets (Fig. 8d).

3.5. Performance under environmental stimuli

The silica capsules were subjected to harsh alkali (0.1 M sodium hydroxide solution) and acid (0.1 M hydrochloric acid solution) treatment to test their stability and responsive behaviour. Such hollow silica microcapsule kept the original morphology after a long period of corrosion (over 120 h) especially in acid solution. It is worth to record that

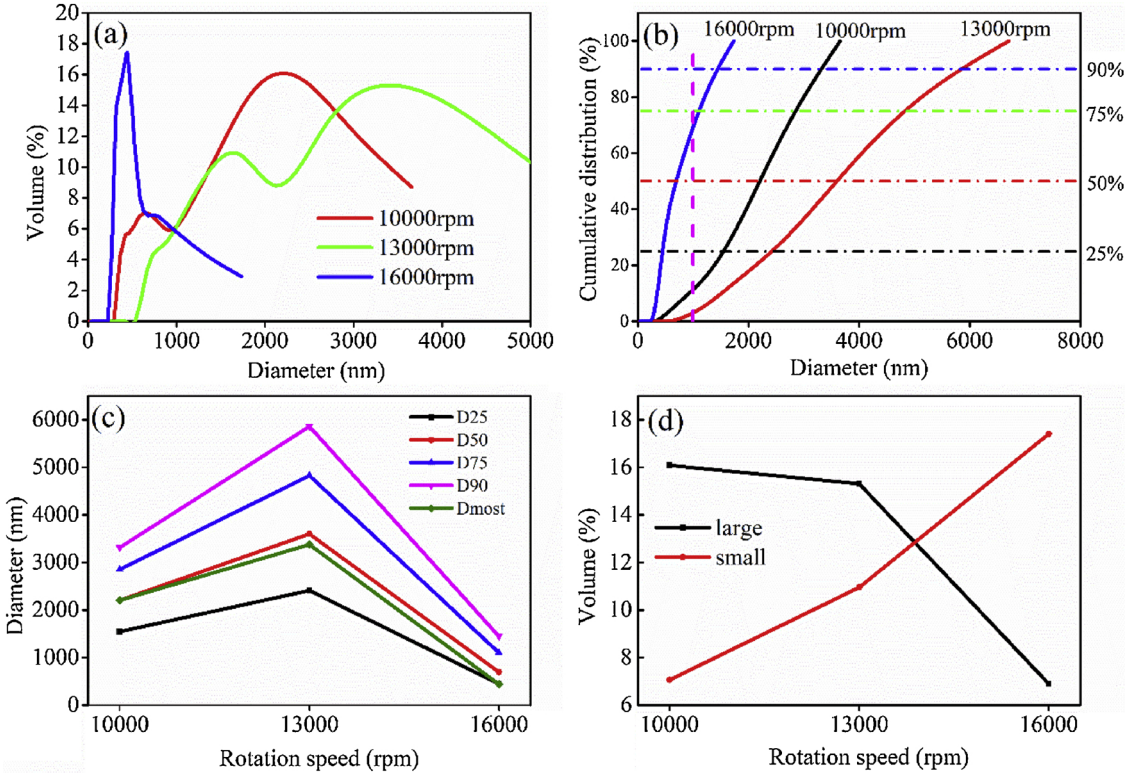

Fig. 8. Curves of (a) diameter distribution, (b) cumulative distribution, (c) diameter versus rotation speed of emulsion and (d) distribution of large and small capsules versus rotation speed.

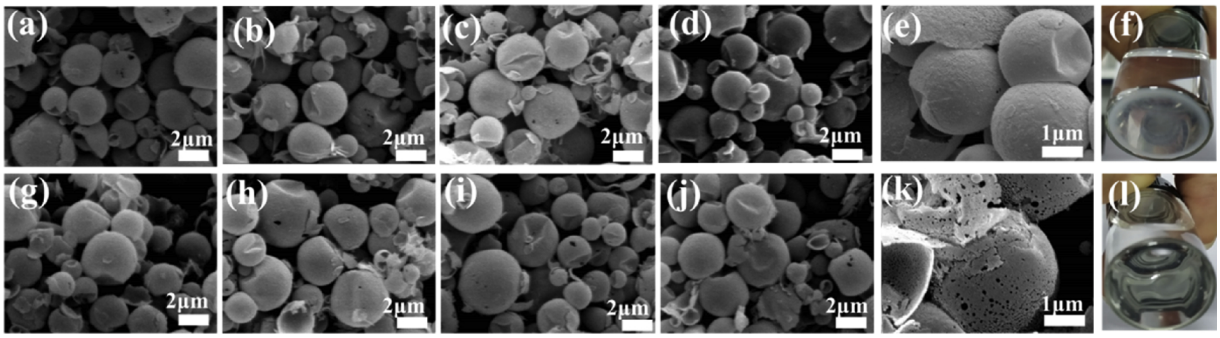

Fig. 9. SEM images after different corrorion time : 10 min, 1 h, 4 h, 24 h, 120 h (a–e for HNO_3 treatment, g–k for NaOH treatment); Photos for bottom of the container under HNO_3 (f) and under NaOH (l).

the amount of silica microcapsules in the alkaline solution was decreasing during harsh alkali treatment for that the silica shell reacted with sodium hydroxide to form solube sodium silicate. In acid solution, there were macroscopic white precipitate gathered at the bottom of the container which were a large quantity of microcapsules. The kinetics process of amorphous silica dissolved in sodium hydroxide is complicated [30], and the reactions that may be involved are showed as following [31,32]:

$$\text{Si-O-Si} + H_2O \rightarrow 2\text{Si-OH} \quad (3)$$

$$\text{Si-OH} + \text{NaOH} \rightarrow \text{Si-O}^- + Na^+ + H_2O \quad (4)$$

$$Si(OH)_4 + 2\text{NaOH} \rightarrow Na_2H_2SiO_4 + 2H_2O \quad (5)$$

There are some defects on outer wall of micromaterials which can be observed in Fig. 9. The Si-O-Si around those defects tend to react faster with the water under alkali environment, and finally form the dissoluble sodium metasilicate. The fragments of microcapsule and holes on shell in Fig. 9 proves this. Such obvious characteristic about response to the alkaline solution is beneficial to the release of rust inhibitor in concrete matrix. The curves of release are as Fig. 10b. In 0.1 M HNO_3 solution, the release platform was found after 72 h. The internal drug may release by free diffusion after a sufficiently long period of time, although the porosity of the microcapsules is not high. In 0.1 M NaOH solution, the time when release rate reached the highest was about 24 h. This indicated that the reaction with silica wall caused by alkaline environment promotes release of drugs in capsules.

Temperature is also worth studying as an important variable in environment. In winter, concrete often cracks due to freeze-thaw cycle. This causes the intrusion of harmful factors such as moisture, chloride ions and carbon dioxide which broke the structure of concrete and damage inner bar. When temperature is below 0 °C, the water will freeze and the volume of ice is larger than the water at liquid state. When the force microcapsule suffered which from distent volume of ice exceeds range of elastic stress that silica shell could bear, crevasses appear and growth. Next, weather get warmer, internal components turn to liquid state and release easily. Broken microcapsules demonstrate the effectiveness of low temperature triggering (Fig S3). Samples were placed in negative temperature environment for 48 h. Such composite structure of water droplet/solid shell is obviously advantageous for the protection of concrete in the region with a large temperature difference. The changes that capsules in different temperature were presented in supporting information. At room temperature, the intact capsules accounted for the majority. However, apart from the hollow microcapsules, there were a large number of fragments and hemispherical capsules under negative temperature conditions. We re-dispersed the microcapsules in an aqueous solution, and measured the content of P and Na in the solution after filtration which were recorded in Fig.10a. The capsules treated at −18 °C released almost 26% more drugs compared to the capsules at room temperature.

4. Conclusion

In summary, we prepared MFP/SiO_2 microcapsules by water in oil emusion soft-template method which achieved direct package of hydrosoluble corrosion inhibitor. Later reinforcement promoted the formation of complete microcapsules and lifted the surface area and roughness as silica was deposited. The concentration of TEOS should be also took into account for that high concentration promote the generation of clavate product, and make the wall of capsules be more thicker. The effect of rotation speed and oil phase volume on capsule size distribution was discussed. Final distribution is the result of equilibrium between droplet break-up and re-coalescence [33]. Coalescence efficiency can be controlled by changing the viscosity which was resulted from dynamic volume fraction. The role rotation speed played was more flexible. High speed at 16,000 rpm tended to form a narrow capsule diameter distribution while wide distribution was observed under slightly mild speed and it turned to be more broad with boosted speed. Low porosity of microcapsule was benificial to ensure drugs'

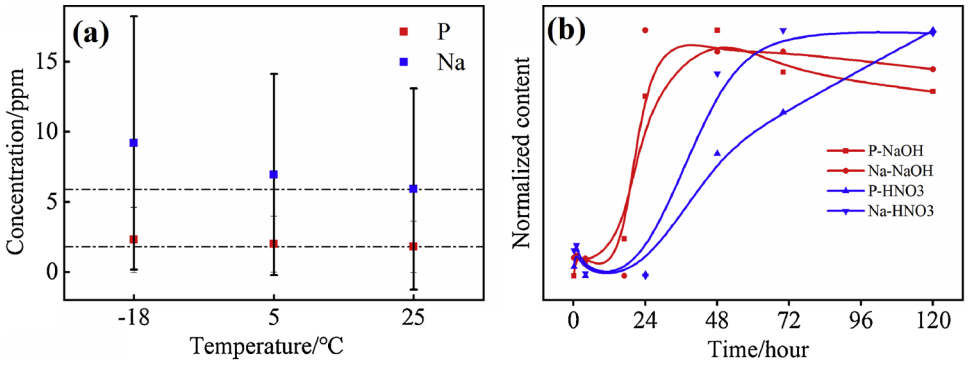

Fig. 10. (a) Concentration of released drugs in aqueous solution for capsules treated in different temperature and (b) Curves of release.

function of corrosion resistance by strengthening water resisting property. This kind of microcapsule is expected to be used in concrete under severe area.

Acknowledgements

The authors would like to acknowledge the financial support from National Key R&D Program of China (No. 2017YFB0406200), “Strategic Priority Research Program” of the Chinese Academy of Science (No. XDA13040505), Science and Technology Service Network Initiative of the Chinese Academy of Sciences (guide project for innovative and entrepreneurial), KFJ-STS-SCYD-112, Key deployment project of the Chinese Academy of Sciences, KFZD-SW-416, Science and Technology Cooperation Project of Sichuan Province and the Chinese Academy of Sciences, 2017JZ0028, and Youth Innovation Promotion Association, CAS (No. 2014288).

Appendix A. Supplementary data

Supplementary data associated with this article can be found, in the online version, at https://doi.org/10.1016/j.colsurfa.2018.11.057.

References

[1] A. Królikowski, J. Kuziak, Impedance study on calcium nitrite as a penetrating corrosion inhibitor for steel in concrete, Electrochim. Acta 56 (23) (2011) 7845–7853.
[2] Yong Ann Ki, Ha-Won Song, Chloride threshold level for corrosion of steel in concrete, Corros. Sci. 49 (11) (2007) 4113–4133.
[3] Han-Seung Lee, Hyun-Min Yang, Jitendra Kumar Singh, Shailesh Kumar Prasad, Bongyoung Yoo, Corrosion mitigation of steel rebars in chloride contaminated concrete pore solution using inhibitor: an electrochemical investigation, Constr. Build. Mater. 173 (2018) 443–451.
[4] T.A. Söylev, M.G. Richardson, Corrosion inhibitors for steel in concrete: state-of-the-art report, Constr. Build. Mater. 22 (4) (2008) 609–622.
[5] Feng Ouyang, Xiaotong Yu, Meng Yuan, Xingguo Feng, Junliang Gao, Chen Da, Na2PO3F as corrosion inhibitor in carbonated cement extract contaminated with chloride ions, Int. J. Electrochem. Sci. 11 (12) (2016) 10620–10627.
[6] Ngala Vt, Page Cl, Page Mm, Corrosion inhibitor systems for remedial treatment of reinforced concrete. Part 2: sodium monofluorophosphate, Corros. Sci. 45 (7) (2003) 1523–1537.
[7] Simon Benita, Microencapsulation: Methods and Industrial Applications, Crc Press, 2005.
[8] Patrick B. Deasy, Microencapsulation and related drug processes, Drugs and Pharmaceutical Sciences, Marcel Dekker, Inc, New York, 1984.
[9] Sy Cheng, Cwm Yuen, Cw Kan, Kkl Cheuk, Development of cosmetic textiles using microencapsulation technology, Res. J. Text. Appar. 12 (4) (2008) 41–51.
[10] Sebastien Gouin, Microencapsulation: industrial appraisal of existing technologies and trends, Trends Food Sci. Technol. 15 (7-8) (2004) 330–347.
[11] Jiandong Zuo, Biqin Dong, Feng Xing, Chaoyun Luo, Dazhu Chen, Preparation of polystyrene/sodium monofluorophosphate microcapsules by W/O/W solvent evaporation method, Adv. Powder Technol. 27 (4) (2016) 1086–1092.
[12] Jiandong Zuo, Jia Zhan, Chaoyun Luo, Biqin Dong, Feng Xing, Dazhu Chen, Characteristics and release property of polylactic acid/sodium monofluorophosphate microcapsules prepared by spray drying, Adv. Powder Technol. 28 (11) (2017) 2805–2811.
[13] Biqin Dong, Weijian Ding, Shaofeng Qin, Chemical self-healing system with novel microcapsules for corrosion inhibition of rebar in concrete, Cem. Concr. Compos. 85 (2018) 83–91.
[14] Stephen B Jaques, Richard D Stehly, Peter B Dunning. Processed silica as a natural pozzolan for use as a cementitious component in concrete and concrete products. Google Patents; 1996.
[15] Use of glass cullet as a cement component in concrete, in: Dyer Td, Dhir Rk (Eds.), Recycling and Reuse of Glass Cullet: Proceedings of International Symposium Dundee UK, 2001.
[16] Rui Liu, Huigang Xiao, Hui Li, et al., Effects of nano-SiO2 on the permeability-related properties of cement-based composites with different water/cement ratios, J. Mater. Sci. 53 (7) (2018) 4974–4986.
[17] Yan Bao, Chunhua Shi, Tong Wang, Xiaolu Li, Jianzhong Ma, Recent progress in hollow silica: Template synthesis, morphologies and applications, Microporous Mesoporous Mater. 227 (2016) 121–136.
[18] S.P. Meaney, R.F. Tabor, B. Follink, Synthesis and characterisation of robust emulsion-templated silica microcapsules, J. Colloid Interface Sci. 505 (2017) 664–672.
[19] Chul Oh, Yong-Geun Lee, Chan-Uk Jon, Oh. Seong-Geun, Synthesis and characterization of hollow silica microspheres functionalized with magnetic particles using W/O emulsion method, Colloids Surf. A: Physicochem. Eng. Asp. 337 (1-3) (2009) 208–212.
[20] Hui Gao, Dongsheng Wen, Gleb B. Sukhorukov, Composite silica nanoparticle/polyelectrolyte microcapsules with reduced permeability and enhanced ultrasound sensitivity, J. Mater. Chem. B 3 (9) (2015) 1888–1897.
[21] Bingyun Sun, Sarah A. Mutch, Robert M. Lorenz, Daniel T. Chiu, Layered polyelectrolyte− silica coating for nanocapsules, Langmuir. 21 (23) (2005) 10763–10769.
[22] Scott C. Warren, Matthew R. Perkins, Ashley M. Adams, et al., A silica sol–gel design strategy for nanostructured metallic materials, Nat. Mater. 11 (5) (2012) 460.
[23] A. Van Blaaderen, J. Van Geest, A. Vrij, Monodisperse colloidal silica spheres from tetraalkoxysilanes: particle formation and growth mechanism, J. Colloid Interface Sci. 154 (2) (1992) 481–501.
[24] Kenneth Sw Sing, Reporting physisorption data for gas/solid systems with special reference to the determination of surface area and porosity (Recommendations 1984), Pure Appl. Chem. 57 (4) (1985) 603–619.
[25] I. Masalova, A. Ya Malkin, Peculiarities of rheological properties and flow of highly concentrated emulsions: the role of concentration and droplet size, Colloid J. 69 (2) (2007) 185–197.
[26] A.A.A. Majid, D.T. Wu, C.A. Koh, New in situ measurements of the viscosity of gas clathrate hydrate slurries formed from model water-in-oil emulsions, Langmuir 33 (42) (2017) 11436–11445.
[27] A.K.L. Oppermann, J.M.E. Noppers, M. Stieger, E. Scholten, Effect of outer water phase composition on oil droplet size and yield of (w1/o/w2) double emulsions, Food Res. Int. 107 (2018) 148–157.
[28] Prudent Placide Anihouvi, Sabine Danthine, Yves Kegelaers, Anne Dombree, Christophe Blecker, Comparison of the physicochemical behavior of model oil-in-water emulsions based on different lauric vegetal fats, Food Res. Int. 53 (1) (2013) 156–163.
[29] S. Carrillo De Hert, T.L. Rodgers, Continuous, recycle and batch emulsification kinetics using a high-shear mixer, Chem. Eng. Sci. 167 (2017) 265–277.
[30] Meriem Fertani-Gmati, Mohamed Jemal, Thermochemical and kinetic investigations of amorphous silica dissolution in NaOH solutions, J. Therm. Anal. Calorim. 123 (1) (2016) 757–765.
[31] Hui Gao, Thaaqib Nazar, Zhongliang Hu, Dongsheng Wen, Gleb B. Sukhorukov, Protective composite silica/polyelectrolyte shell with enhanced tolerance to harsh acid and alkali conditions, J. Colloid Interface Sci. 512 (2018) 198–207.
[32] Yuichi Niibori, Masahisa Kunita, Osamu Tochiyama, Tadashi Chida, Dissolution rates of amorphous silica in highly alkaline solution, J. Nucl. Sci. Technol. 37 (4) (2000) 349–357.
[33] Seid Mahdi Jafari, Elham Assadpoor, Yinghe He, Bhesh Bhandari, Re-coalescence of emulsion droplets during high-energy emulsification, Food Hydrocoll. 22 (7) (2008) 1191–1202.